Inferences from the ^{1}H-NMR Spectroscopic Study of an Antiferromagnetically Coupled Heterobinuclear Fe(III)−(X)−Cu(II) $S = 2$ Spin System (X = O^{2-}, OH^-)

Alaganandan Nanthakumar, Stephen Fox,† Narasimha N. Murthy,‡ and Kenneth D. Karlin*

Contribution from the Department of Chemistry, The Johns Hopkins University, Charles & 34th Streets, Baltimore, Maryland 21218

Received July 12, 1996[⊗]

Abstract: This study considers how the electronic relaxation rate enhancement effects of strong antiferromagnetic coupling in the $Fe^{III}-X-Cu^{II}$ unit (X = O^{2-}, OH^-) of complexes $[(F_8\text{-TPP})Fe^{III}-O-Cu^{II}(TMPA)]^+$ (**1**), and $[(F_8\text{-TPP})Fe^{III}-OH-Cu^{II}(TMPA)]^+$ (**2**) (F_8-TPP = tetrakis(2,6-difluorophenyl)porphyrinate(2−); TMPA = tris(2-pyridylmethyl)amine) are manifested as observable upfield-shifted resonances of the TMPA moiety in the ^{1}H-NMR spectra. The pyrrole resonances appear at 65 and 69 ppm, respectively, for **1** and **2**, consistent with an $S = 2$ ground state derived from antiferromagnetic coupling of high-spin Fe^{III} ($S = 5/2$) and Cu^{II} ($S = 1/2$) through the bridging ligand X. Paramagnetic mononuclear complexes $[Co(TMPA)(CH_3CN)]^{2+}$ ($S = 3/2$) (X-ray structure reported) and $[Cu(TMPA)(CH_3CN)]^{2+}$ ($S = 1/2$) demonstrate downfield-shifted peaks consistent with a σ contact shift mechanism. Assignments for all complexes were achieved via ^{1}H- and ^{2}H-NMR spectroscopy of appropriately synthesized methylated and deuteriated derivatives. In $[Cu(TMPA)(CH_3CN)]^{2+}$, the observed ligand peaks (298 K) are broad; in **1**, however, they are considerably sharper and upfield-shifted to −61, −7, 4.5, −21, and −104 ppm, corresponding to pyridyl 6-H, 5-H, 4-H, and 3-H and aminomethyl $-CH_2-$, respectively, of TMPA. The observance of these upfield peaks is a consequence of enhancement of the electronic relaxation rate for Cu^{II} due to antiferromagnetic coupling with the faster relaxing Fe^{III}. This observation represents the prototype of a $Fe^{III}-X-Cu^{II}$ $S = 2$ spin state hitherto only theoretically predicted. The attenuation of δ for a particular hydrogen as its distance (through bonds) from Cu^{II} increases correlates with a σ contact shift mechanism. Only one peak per type of pyridyl H is observed (from 220 to 300 K for **1** and from 220 to 270 K for **2**), indicating dynamic behavior of the Cu−TMPA moiety in solution. Both **1** and **2** exhibit pseudo-Curie temperature dependence manifested as augmentation of δ in both upfield and downfield directions as temperature is lowered. Linear Curie and anti-Curie plots of the pyrrole and TMPA chemical shifts (from 220 to 300 K for **1** and from 220 to 270 K for **2**) imply a *predominantly* $S = 2$ spin state in each case; i.e., the extent of antiferromagnetic coupling is *strong*.

Introduction

Interest in the NMR spectroscopy of paramagnetic metal complexes, either in metalloproteins or small molecules, has expanded considerably in recent years, owing to an increasing understanding of theory, and application of techniques, derived from a variety of systems.[1] For example, the chemical shift for iron−porphyrinate complexes has been found to correlate with the oxidation state and spin state of the metal,[2] rendering a potentially important basis for the interpretation of the NMR properties of heme proteins.[3] Although ^{1}H-NMR spectra of mononuclear Cu(II) complexes are typically precluded on account of slow electronic relaxation and subsequent broad, irresolvable lines, examples of magnetically-coupled Cu(II)···Cu(II) dimers and correlations of chemical shift, line width, and nature of magnetic interactions are emerging.[4]

In paramagnetic complexes, the interaction of metal-centered unpaired spin density with protons of the ligands gives rise to the observed chemical shifts, as a sum of contact (through bonds), dipolar (through space), and diamagnetic terms. In high-spin iron(III) tetraphenylporphyrins and mononuclear Cu complexes, the contact shift contribution dominates the overall chemical shift.[5,6] Dipolar shifts are dominant in metal complexes such as square-planar cobalt(II) and iron(II) porphyrins, which have unpaired electrons in orbitals lacking contact delocalization pathways; these molecules generally have large magnetic anisotropy.[5]

* To whom correspondence should be addressed. Phone: (410) 516-8027. Fax: (410) 516-6164 (or 8420). E-mail: karlin@jhuvms.hcf.jhu.edu.

† Current address: Chemistry Department, Northeast Louisiana University, Monroe, LA 71209.

‡ Current address: Department of Chemistry, IIT Madras, Madras 600 036, India.

⊗ Abstract published in *Advance ACS Abstracts,* March 1, 1997.

(1) (a) Bertini, I.; Turano, P.; Vila, A. J. *Chem. Rev.* **1993**, *93*, 2833−2932. (b) Bertini, I.; Turano, P. In *NMR of Paramagnetic Molecules*; La Mar, G. N., Ed.; Kluwer Academic: Dordrecht, The Netherlands, 1994. (c) Bertini, I.; Luchinat, C. *NMR of Paramagnetic Molecules in Biological Systems*; Benjamin Cummings: Menlo Park, CA, 1986. (d) Bertini, I.; Luchinat, C. *NMR of Paramagnetic Substances*; Elsevier: Amsterdam, 1996.

(2) (a) Scheidt, W. R.; Reed, C. A. *Chem. Rev.* **1981**, *81*, 543−555. (b) Walker, F. A.; Simonis, U. In *Biological Magnetic Resonance*; Berliner, J., Reuben, J., Eds.; Plenum: New York, 1993; pp 133−274. (c) La Mar, G. N.; Horrocks, W. D.; Holm, R. H. *NMR of Paramagnetic Molecules*; Academic Press: New York, 1983; Vol. 2, pp 187−257. (d) Goff, H. M. In *Iron Porphyrins*; Lever, A. P. B., Gray, H. B., Eds.; Addison-Wiley: Reading, MA, 1983; Vol. Part 1; Chapter 4.

(3) (a) La Mar, G. N.; de Ropp, J. S. In *Biological Magnetic Resonance*; Berliner, J., Reuben, J., Eds.; Plenum: New York, 1993; pp 1−78. (b) Satterlee, J. D.; Alam, S.; Yi, Q.; Erman, J. E.; Constantinidis, I.; Russell, D. J.; Moench, S. J. In *Biological Magnetic Resonance*; Berliner, J., Reuben, J., Eds.; Plenum: New York, 1993; pp 275−298.

(4) (a) Holz, R. C.; Brink, J. M. *Inorg. Chem.* **1994**, *33*, 4609−4610. (b) Satcher, J. H.; Balch, A. L. *Inorg. Chem.* **1995**, *34*, 3371−3373. (c) Mandal, P. K.; Manoharan, P. T. *Inorg. Chem.* **1995**, *34*, 270−277. (d) Benelli, C.; Dei, A.; Gatteschi, D. *Inorg. Chem.* **1982**, *21*, 1284−1286. (e) Murthy, N. N.; Karlin, K. D.; Bertini, I.; Luchinat, C. *J. Am. Chem. Soc.* **1997**, *119*, 2156−2162.

(5) Bertini, I.; Luchinat, C. In *Physical Methods for Chemists*, 2nd ed.; Drago, R. S., Ed.; Harcourt Brace Jovanovich: Orlando, FL, 1992; pp 500−556.

(6) Bertini, I.; Dei, A.; Scozzafava, A. *Inorg. Chem.* **1975**, *14*, 1526−1528.

S0002-7863(96)02404-3 CCC: $14.00

Scheme 1

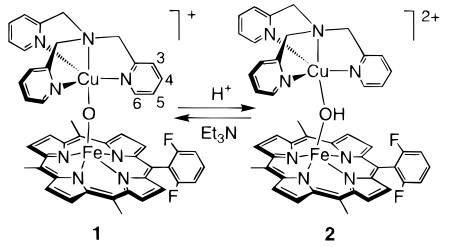

We are investigating small-molecule analogues for the porphryin−iron/copper binuclear center in heme−copper oxidases.[7] This center is directly involved in O_2-binding and reduction (to water), as well as mediating the membrane proton-translocation process, the primary function of these enzymes. Via reaction of O_2 with reduced complexes or through acid−base self-assembly chemistry, we have generated complex [(F_8-TPP)Fe^{III}−O−Cu^{II}(TMPA)]$^+$ (**1**) (F_8-TPP = tetrakis(2,6-difluorophenyl)porphyrinate(2−); TMPA = tris(2-pyridylmethyl)amine) (Scheme 1).[8−10] This oxo-bridged compound **1** has short Fe−O and Cu−O bonds (1.740(5) Å and 1.856(5) Å, respectively) which are essentially colinear (∠Fe−O−Cu = 178.2(4)°). Detailed Mössbauer and magnetic studies of **1** led to the assignment of a high-spin Fe(III) ($S = 5/2$) ion, which is antiferromagnetically-coupled to Cu(II) to constitute an overall $S = 2$ electronic ground state with $J = -87$ cm^{-1} (where $H = -2JS_1 \cdot S_2$) for **1** in the solid state.[8] Complex **1** is quite basic: the μ-oxo group can be reversibly protonated to give [(F_8-TPP)Fe^{III}−OH−Cu^{II}(TMPA)]$^{2+}$ (**2**) (Scheme 1), which possesses elongated Fe−O(H) (1.87 ± 0.02 Å) and Cu−O(H) (1.89 ± 0.02 Å) bonds; the hybridization change at the bridging oxygen atom results in a substantial bending such that ∠Fe−O(H)−Cu = 157 ± 5°.[10]

In our early characterization of **1**,[8−10] we noted its striking ^{1}H-NMR spectroscopic properties (at 298 K): in addition to the expected signals of the porphyrinate phenyl protons in the 7−12 ppm region, we observed an unusually placed pyrrole resonance at 65 ppm, and dramatically upfield-shifted signals (at −7, −21, and −104 ppm) which we attributed to the TMPA ligand protons. This range of shifts is unprecedented at room temperature in heterobinuclear coordination complexes; although upfield shifts are reported for mixed-valent Fe_4S_4 (HiPiP) cubanes (i.e., up to −35 ppm),[11,12,13a,b] model compounds for iron−sulfur proteins,[14] and Co(II)-substituted (for Zn(II)) Cu−Zn superoxide-dismutase (SOD),[12,15] they are not easily distinguishable due to the complexity of the systems and smaller coupling/effective magnetic moment. In Co(II)-substituted SOD, antiferromagnetic coupling promotes enhancement of the electron-relaxation rate at the Cu(II) site; this results in line narrowing such that the Cu(II)-ligand protons become observable.[13c−e,15] Furthermore, at lower temperatures, these Cu(II)-ligand protons become upfield-shifted,[13] owing to the increased population of the $S = 1$ ground state, and the resulting increase in the negative coefficient (discussed below) contribution to the isotropic shift ensuing from the antiferromagnetic coupling of two unlike paramagnetic metal ions.[12,16] Complexes **1** and **2** offer the first examples of heterobinuclear $S = 2$ copper-containing synthetic or biological complexes, which, on account of their inherent strong coupling, succinctly illustrate the upfield- and downfield-shifted peak "signature" [12] over an unprecedentedly large chemical shift range, and, in the case of **1**, at ambient temperature.

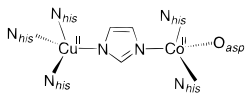

Thus, we have undertaken a detailed evaluation of the ^{1}H-NMR spectroscopic properties of [(F_8-TPP)Fe^{III}−O−Cu^{II}-(TMPA)]$^+$ (**1**) and [(F_8-TPP)Fe^{III}−OH−Cu^{II}(TMPA)]$^{2+}$ (**2**). This includes the complete chemical shift assignment for all resonances observed or expected for **1**. To accomplish this, the TMPA ligand was separately derivatized with a methyl group at the pyridyl 3-, 4-, and 5-positions, and deuteriated at the pyridyl 6-position, and the methylene of the tripod arm; analogues of **1** were then synthesized, and spectra determined. To obtain further insights and supporting information, the temperature dependence of the ^{1}H-NMR spectra of **1** and **2** have been acquired, and a cobalt(II) complex, [Co^{II}(TMPA)(CH_3CN)]$^{2+}$, as a paramagnetic NMR spectroscopic analogue of the [Cu^{II}-(TMPA)] portion of **1**, has been synthesized and characterized.

Experimental Section

Synthesis, Materials, and Methods. Reagents and solvents used were of commercially available reagent quality unless otherwise stated. Dichloromethane (CH_2Cl_2) was stirred with concentrated sulfuric acid for several days and washed with water, sodium carbonate (10%) solution, and water. It was then dried over anhydrous $MgSO_4$ and CaH_2 before a final reflux and distillation from CaH_2. Acetonitrile (CH_3-CN) was distilled from CaH_2. Anhydrous diethyl ether was prepared by passing reagent-grade solvent through a column of activated alumina. Preparation and handling of air-sensitive materials were carried out under an argon atmosphere using standard Schlenk techniques. Solid samples were stored and transferred, and samples for IR and NMR spectra were prepared, in a Vacuum Atmospheres drybox filled with nitrogen.

Elemental analyses were performed by National Chemical Consulting, Tenafly, NJ, and Desert Analytics, Tucson, AZ. Infrared spectra were recorded as Nujol mulls on a Mattson Galaxy FTIR spectrometer. Electronic spectra were recorded on a Shimadzu UV 160U instrument. All wavelengths are reported in nanometers, and the molar extinction coefficients are listed in parentheses. Proton, deuterium, and T_1 NMR measurements were obtained using a Bruker 300 MHz instrument. The T_1 values were measured using an inversion recovery (180−τ−90)

(7) (a) Iwata, S.; Ostermeier, C.; Ludwig, B.; Michel, H. *Nature* **1995**, *376*, 660−669. (b) Tsukihara, T.; Aoyama, H.; Yamashita, E.; Tomizaki, T.; Yamaguchi, H.; Shinzawa-Itoh, K.; Nakashima, R.; Yaono, R.; Yoshikawa, S. *Science* **1995**, 1069−1074. (c) Solomon, E. I.; Sundaram, U. M.; Machonkin, T. E. *Chem. Rev.* **1996**, *96*, 2563−2605

(8) Karlin, K. D.; Nanthakumar, A.; Fox, S.; Murthy, N. N.; Ravi, N.; Huynh, B. H.; Orosz, R. D.; Day, E. P. *J. Am. Chem. Soc.* **1994**, *116*, 4753−4763.

(9) Nanthakumar, A.; Fox, S.; Murthy, N. N.; Karlin, K. D.; Ravi, N.; Huynh, B. H.; Orosz, R. D.; Day, E. P.; Hagen, K. S.; Blackburn, N. J. *J. Am. Chem. Soc.* **1993**, *115*, 8513−8514.

(10) Fox, S.; Nanthakumar, A.; Wikström, M.; Karlin, K. D.; Blackburn, N. J. *J. Am. Chem. Soc.* **1996**, *118*, 24−34.

(11) Bertini, I.; Briganti, F.; Luchinat, C.; Scozzafava, A.; Sola, M. *J. Am. Chem. Soc.* **1991**, *113*, 1237−1245.

(12) Luchinat, C.; Ciurli, S. In *Biological Magnetic Resonance*; Berliner, J., Reuben, J., Eds.; Plenum: New York, 1993; pp 357−420.

(13) (a) Bertini, I.; Owens, C.; Luchinat, C.; Drago, R. S. *J. Am. Chem. Soc.* **1987**, *109*, 5208−5212. (b) Bertini, I.; Luchinat, C.; Messori, L.; Vasak, M. *J. Am. Chem. Soc.* **1989**, *111*, 7296−7300. (c) Bertini, I.; Banci, L.; Brown, R. D.; Koenig, S. H.; Luchinat, C. *Inorg. Chem.* **1988**, *27*, 951−953. (d) Banci, L.; Bertini, I.; Luchinat, C.; Scozzafava, A. *J. Am. Chem. Soc.* **1987**, *109*, 2328−2334. (e) Bertini, L.; Lanini, G.; Luchinat, C.; Messori, L.; Monnanni, R.; Scozzafava, A. *J. Am. Chem. Soc.* **1985**, *107*, 4391−4396. (f) Bertini, I.; Briganti, F.; Luchinat, C.; Scozzafava, A. *Inorg. Chem.* **1990**, *29*, 1874−1880. (g) Banci, L.; Bertini, I.; Briganti, F.; Luchinat, C.; Scozzafava, A. *Inorg. Chem.* **1991**, *30*, 4517−4524.

(14) Ciurli, S.; Yu, S.-b.; Holm, R. H.; Srivastava, K. K. P.; Münck, E. *J. Am. Chem. Soc.* **1990**, *112*, 8169−8171.

(15) (a) Bertini, I.; Luchinat, C.; Piccioli, M. *Progress in NMR Spectroscopy*; Elsevier: Oxford, 1994; pp 91−139. (b) Banci, L. In *Biological Magnetic Resonance*; Berliner, J., Reuben, J., Eds.; Plenum: New York, 1993; pp 79−111.

(16) Upfield shifting with lower temperature is also observed for the reduced form of Fe_2S_2 (Fe(III)···Fe(II)) ferredoxins.[5,12]

Scheme 2

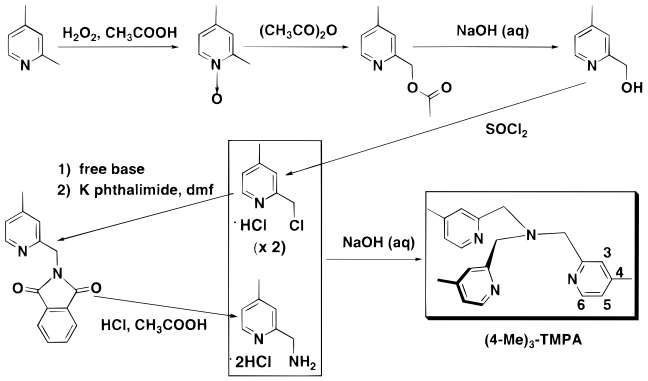

method. Chemical shifts are reported as δ values downfield from an internal standard, Me_4Si.

TMPA,[17] **[Cu(TMPA)(CH$_3$CN)][ClO$_4$],**[17] **(F$_8$-TPP)Fe−OH,**[8] **[(F$_8$-TPP)Fe−O−Cu(TMPA)][ClO$_4$],**[8] **and [(F$_8$-TPP)Fe−OH−Cu(TMPA)][ClO$_4$]$_2$**[10] were synthesized according to published procedures.

Full details of the synthesis of deuteriated or methylated tmpa ligands, deuteriated porphyrins, and copper, porphyrinate−iron or Fe−O(H)−Cu complexes are given in the Supporting Information.

In Situ ^{1}H-NMR Spectra of (*n*-Me)$_3$-TMPA Complexes of Co(II). In a small vial was prepared a solution of the respective (*n*-Me)$_3$-TMPA (n = 3, 4, and 5) ligand (0.033 g, 0.1 mmol) (Supporting Information) and Co(II)(ClO$_4$)$_2$·6H$_2$O (0.037 g, 0.1 mmol) in CD$_3$CN (0.5 mL). The brown solution was then transferred via pipet to an NMR tube, and the spectra were recorded.

X-ray Structure of [(TMPA)Co(II)(CH$_3$CN)](ClO$_4$)$_2$. Full details for the X-ray structure determination are given in the Supporting Information; this includes experimental details, listing of atomic coordinates, temperature factors, and anisotropic temperature factors, and tables of bond lengths and bond angles.

Results and Discussion

Ligands. The methyl-substituted series (*n*-Me)$_3$-TMPA (n = 3, 4, and 5) was prepared, in gram quantities for each ligand; the synthesis of (4-Me)$_3$-TMPA, for example, and the numbering protocol for TMPA are illustrated in Scheme 2. Further details are given in the Experimental Section or Supporting Information.

Mononuclear Copper(II) and Cobalt(II) Complexes. The Cu(II) complexes of the tetradentate (*n*-Me)$_3$-TMPA (n = 3, 4, and 5) ligands were isolated as perchlorate salts in good yield (>70%), as blue crystalline solids from CH$_3$CN/diethyl ether. There are slight but distinct differences (vide infra) in the electronic spectra (CH$_3$CN) of the series [Cu(*n*-Me)$_3$-TMPA]$^{2+}$ (n = 3, 4, and 5); their absorptions appear in the range 845−870 nm as a low-intensity peak ($\epsilon \approx 250$), with a high-energy shoulder around 550 nm, expected for the two d−d transitions of trigonal-bipyramidal Cu(II).[17,18] We assign the "fifth" ligand in solution to coordinated CH$_3$CN.

The [Co(TMPA)(CH$_3$CN)]$^{2+}$ complex was prepared in a similar manner, with comparably good yield, as a brown crystalline solid. The X-ray crystal structure of [Co(TMPA)(CH$_3$CN)][ClO$_4$]$_2$ (Figure 1) indicates that the pyridyls are arranged in a pseudo-3-fold symmetric manner (Co−N distances 2.04−2.05 Å). The relatively long Co−N(apical amine) distance of 2.177 Å (3) forces the Co(II) out of the equatorial plane, toward the nitrile ligand by 0.390 Å, slightly distorting

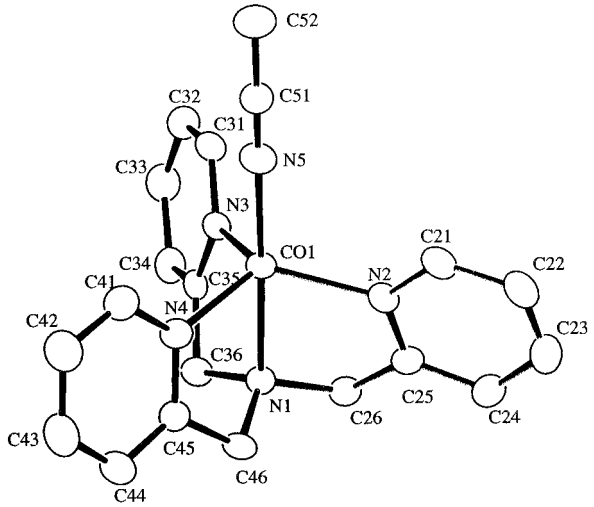

Figure 1. ORTEP view (20% ellipsoids) of [Co(TMPA)(CH$_3$CN)]$^{2+}$.

Scheme 3

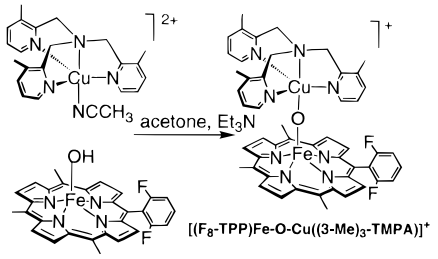

the molecule from ideal trigonal-bipyramidal geometry (TBP); the empirical structure value τ for this complex is 0.94 (1.00 for TBP, 0.00 for square-pyramidal).[19] The solution magnetic moment (Evans method) of [Co(TMPA)(CH$_3$CN)][ClO$_4$]$_2$ at 298 K (μ_B = 4.16) is consistent with an S = 3/2 spin state, and trigonal-bipyramidal high-spin Co(II).

Similarly, in the crystal structure of [Cu(TMPA)(CH$_3$CN)][ClO$_4$]$_2$,[17] the Cu(II) is displaced toward the axial nitrile ligand by 0.279 Å; again, the pyridyls are symmetrically coordinated, (Cu−N distances 2.02−2.08 Å), with the planes of the pyridine ring essentially perpendicular to the *xy*-plane. The τ value for this complex is 0.96.[19]

Synthesis of [(F$_8$-TPP)Fe−O−Cu((*n*-Me)$_3$-TMPA)]$^+$ Complexes. The [(F$_8$-TPP)Fe−O−Cu((3-Me)$_3$-TMPA)]$^+$ complex precipitated as microcrystals directly from the acetone reaction mixture in >70% yield, by the same acid-base strategy previously reported for the synthesis of [(F$_8$-TPP)Fe−O−Cu(TMPA)]$^+$ (Scheme 3).[10] Although electronic spectra of the crude reaction mixtures demonstrated essentially quantitative generation of [(F$_8$-TPP)Fe−O−Cu((*n*-Me)$_3$-TMPA)]$^+$ (n = 3, 4, and 5), the greater solubility of the 4-Me and 5-Me analogs resulted in their somewhat lower isolated yields (20−40%), these complexes ultimately being obtained as toluene solvates by recrystallization from CH$_2$Cl$_2$/toluene.

Electronic spectra of the μ-oxo complexes [(F$_8$-TPP)Fe−O−Cu((*n*-Me)$_3$-TMPA)]$^+$ (n = 3, 4, and 5) are essentially invariant, each displaying the characteristic red-shifted Soret band at 434 nm, and α-band at 554 nm, identical with the parent complex [(F$_8$-TPP)Fe−O−Cu(TMPA)]$^+$ (**1**).[8,10] Not surprisingly, the slight electronic differences observed in the [Cu((*n*-Me)$_3$-TMPA)(CH$_3$CN)]$^{2+}$ (n = 3, 4, and 5) complexes (vide supra) do not appear to influence the porphyrin-dominated UV−vis features of the corresponding μ-oxo complexes [(F$_8$-TPP)Fe−O−Cu((*n*-Me)$_3$-TMPA)]$^+$.

(17) (a) Tyeklár, Z.; Jacobson, R. R.; Wei, N.; Murthy, N. N.; Zubieta, J.; Karlin, K. D. *J. Am. Chem. Soc.* **1993**, *115*, 2677−2689. (b) Jacobson, R. R. Ph.D. Dissertation, State University of New York at Albany, 1989.

(18) (a) Wei, N.; Murthy, N. N.; Karlin, K. D. *Inorg. Chem.* **1994**, *33*, 6093−6100. (b) Hathaway, B. J. In *Comprehensive Coordination Chemistry*; Wilkinson, G., Ed.; Pergamon: New York, 1987; Vol. 5, pp 533−774. (c) Thompson, L. K.; Ramaswamy, B. S.; Dawe, R. D. *Can. J. Chem.* **1978**, *56*, 1311.

(19) Addison, A. W.; Rao, T. N.; Reedijk, J.; van Rijn, J.; Verschoor, G. C. *J. Chem. Soc., Dalton Trans.* **1984**, 1349−1356.

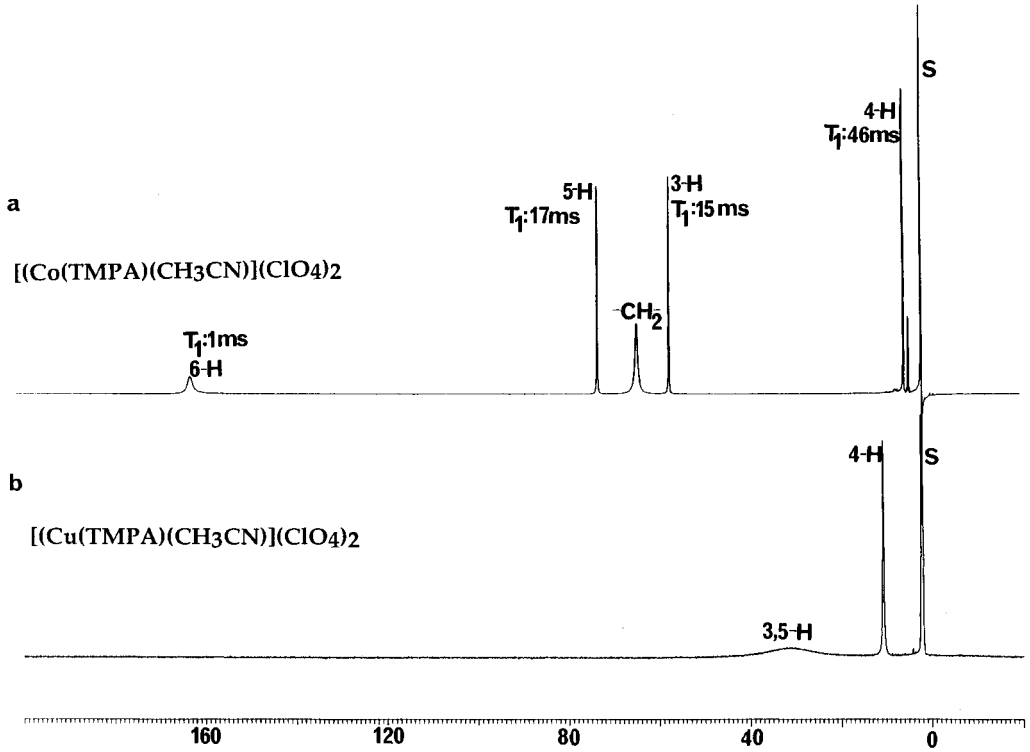

Figure 2. Comparison of ^{1}H-NMR spectra of the $[Co(TMPA)(CH_3CN)](ClO_4)_2$ complex and $[Cu(TMPA)(CH_3CN)](ClO_4)_2$ in CD_3CN.

Table 1. Comparison of Chemical Shifts (ppm) in ^{1,2}H-NMR Spectra of $[Cu(TMPA)CH_3CN]^{2+}$, $[(F_8\text{-TPP})Fe-O-Cu(TMPA)]^+$, and Their Methyl-Substituted and Deuteriated TMPA Derivatives at 298 K, in CD_3CN Unless Noted

^{1}H-NMR Spectra

	peak positions (ppm)								
$[Cu((3\text{-}Me)_3\text{-}TMPA)(CH_3CN)]^{2+}$	31.4	10.4	2.4						
$[Cu((4\text{-}Me)_3\text{-}TMPA)(CH_3CN)]^{2+}$	29.0		−2.0						
$[Cu((5\text{-}Me)_3\text{-}TMPA)(CH_3CN)]^{2+}$	31.7	10.2	6.4						
$[Cu(TMPA)(CH_3CN)]^{2+}$	30.0	10.6							
assignment	3, 5-H	4-H	Me						
$[Co(TMPA)(CH_3CN)]^{2+}$	162	73	64	57	6				
$[Co(TMPA)]^{2+}(CD_2Cl_2)$	170	71	119	52	19				
assignment	6-H	5-H	$-CH_2-$	3-H	4-H				
$[(F_8\text{-TPP})Fe-O-Cu(TMPA)]^+$	65	9.6, 9.2		7.6	4.5	−7	−21	−104	
$[(F_8\text{-TPP})Fe-O-Cu((3\text{-}Me)_3\text{-}TMPA)]^+$	65	9.6, 9.2		7.6	4.5	−7		−104	2
$[(F_8\text{-TPP})Fe-O-Cu((4\text{-}Me)_3\text{-}TMPA)]^+$	65	9.6, 9.2		7.6		−7	−21	−104	7
$[(F_8\text{-TPP})Fe-O-Cu((5\text{-}Me)_3\text{-}TMPA)]^+$	65	9.6, 9.2		7.6	4.5		−21	−104	0
$[(F_8\text{-TPP})Fe-O-Cu(TMPA)]^+$ (250 K, CD_2Cl_2)	78	9.7, 9.5		7.7		−10	−28	−125	
$[(F_8\text{-TPP})Fe-OH-Cu(TMPA)]^{2+}$ (250 K, CD_2Cl_2)	81	12.5, 11.6		7.9	3.4	−14	−25	−132	
assignment	pyrr	*m*-phenyl		*p*	4-H	5-H	3-H	$-CH_2-$	Me

^{2}H-NMR Spectra

	peak positions			peak positions	
$[(F_8\text{-TPP-}d_8)Fe-O-Cu((-CH_2-)\text{-TMPA})]^+$	65		$[(F_8\text{-TPP-}d_8)Fe-O-Cu((-CD_2-)\text{-TMPA})]^+$	65	−104
assignment	pyrr		assignment	pyrr	$-CD_2-$
$[(F_8\text{-TPP-}d_8)Fe-O-Cu((6\text{-D})\text{-TMPA})]^+$	65	−61			
assignment	pyrr	6-D			

^{1}H-NMR Spectra of Mononuclear Cobalt(II) Complexes. If we consider the trigonal-bipyramidal structure of $[Co(TMPA)(CH_3CN)]^{2+}$ (Figure 2) to be retained in CD_3CN solution, the unpaired electrons ($S = 3/2$) reside in the equatorially-oriented degenerate d_{xy} and $d_{x^2-y^2}$, and axially-oriented d_{z^2} orbitals, all of which can delocalize unpaired-spin via σ bonds. The π orbitals of the pyridyls are orthogonal to d_{z^2}, but can achieve some overlap with d_{xy} and $d_{x^2-y^2}$ to afford additional π delocalization. The origin of the considerably downfield-shifted ^{1}H-NMR spectrum of $[Co(TMPA)(CH_3CN)]^{2+}$ (Figure 2), therefore, is largely attributed to a σ contact shift mechanism, which is precedented for Co(II)−pyridyl complexes.[5]

For high-spin Co(II) complexes, the short electronic relaxation time ($\tau_s \approx 10^{-11}$ s) for Co(II) results in relatively sharp proton NMR signals.[13] Accordingly, the ^{1}H NMR spectrum of $[Co(TMPA)(CH_3CN)]^{2+}$ in CD_3CN shows five distinct features (Table 1), in the range 0−162 ppm, ascribable to the TMPA pyridyl and methylene protons. The methylene protons were assigned by deuteriation; they appear as a broad peak at 64 ppm. The 5-H, 3-H, and 4-H pyridyls were assigned by methylation to $\delta = 71$, 55, and 5 ppm, respectively; their T_1 measurements were 71 ppm ($T_1 = 17$ ms), 55 ppm ($T_1 = 15$ ms) and 5 ppm ($T_1 = 36$ ms). Assuming a dominant dipolar relaxation mechanism (since T_1 is dependent only on the distance between

the metal and proton), this attenuation of T_1 with distance from the metal supports the notion of a dominant σ contact shift mechanism.[5] On these grounds, we assign the furthest shifted peak at 162 ppm ($T_1 = 1$ ms) to the proton closest to the Co(II): the 6-pyridyl proton.

It is of interest that, in the ^{1}H-NMR spectrum of [Co(TMPA)(CH$_3$CN)]$^{2+}$ dissolved in CD_2Cl_2, the methylene peak moves dramatically to 119 ppm (a shift of 55 ppm), whereas the other peaks move correspondingly much less (Table 1). We attribute this to the effective loss of axial nitrile ligation in CD_2Cl_2, which forces more σ contact spin density to be transmitted through the d_{z^2} lobes on to the methylene tripod arm, resulting in the large downfield shift.

^{1}H-NMR Spectra of Mononuclear Cu(II) Complexes. For mononuclear copper(II) complexes, ^{1}H-NMR signals are generally not observed owing to the relatively long electronic relaxation time ($\tau_s \approx 10^{-9}$ s) for Cu^{2+},[4d,e,5,13c−e] which leads to line broadening. The ^{1}H-NMR spectrum of [Cu(TMPA)(CH$_3$CN)]$^{2+}$ in CD_3CN, however (Figure 2), shows distinct features which we now assign on the basis of comparisons within the series of (*n*-Me)$_3$-TMPA ($n = 3$, 4, and 5) complexes (Table 1). All complexes except [Cu((4-Me)$_3$-TMPA)(CH$_3$CN)]$^{2+}$ show a relatively sharp resonance at ~10.5 ppm (Figure S1, Supporting Information); this absorption therefore originates from the pyridyl 4-H, which is furthest removed from the paramagnetic metal center. In addition, all complexes exhibit a very broad "peak" around 30 ppm; since it appears to be narrower for the individual 3-Me- and 5-Me-substituted derivatives, we deduce that this feature originates from the pyridyl 3-H and 5-H atoms *together*. This attenuation of chemical shift with number of bonds distance from the metal is consistent with a σ contact shift mechanism, as is expected for Cu(II) complexes.[6]

We note that peaks ascribable to the methyl groups of the substituted TMPA ligands do appear, as given in Table 1. The relative upfield shift of the 4-Me ($\delta \approx -2$ ppm) vs the 3-Me ($\delta \approx 2.4$ ppm) and 5-Me ($\delta \approx 6.4$ ppm) is accounted for by the one bond further removal from the metal center in the case of the 4-Me, which results in a diminished σ contribution to the contact shift, and perhaps allows a π contribution to predominate at this position (vide infra).[20]

The closest protons to the Cu center, the methylene and 6-pyridyl protons, were not detectable; in fact, even deuteriation of these positions, and subsequent ^{2}H NMR, failed to distinguish any signals. For reasons to be discussed, this approach *was* successful in the detection and assignment of the methylene and 6-pyridyl TMPA protons in [(F$_8$-TPP)Fe−O−Cu(TMPA)]$^+$ (**1**).

In trigonal-bipyramidal [Cu(TMPA)(CH$_3$CN)]$^{2+}$ the only unpaired spin formally resides in the d_{z^2} orbital, which can delocalize by a σ contact shift through the axial bonds. In addition, we visualize the σ transmission of unpaired spin into the *xy*-plane through the d_{z^2} "torus", and/or by mixing of s character into the d_{z^2} orbital. We observe the order of shift to be 3-H ≈ 5-H > 4-H (Table 1), which strongly suggests that the contact shift must be operating principally in the *xy*-plane via the the Cu−N(pyridyl) bonds. Since the d_{z^2} lobes are orthogonal to the π orbitals of the pyridyls, we anticipate only nominal π delocalization, although this appears to be significant where σ contact shift has "decayed," for instance, at the 4-Me position (vide supra).

^{1}H- and ^{2}H-NMR Spectroscopic Assignments for [(F$_8$-TPP)Fe−O−Cu(TMPA)](ClO$_4$). The complete assignments

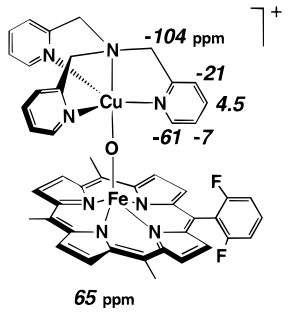

Figure 3. Summary of ^{1}H-NMR assignments for [(F$_8$-TPP)Fe−O−Cu(TMPA)]$^+$ (**1**).

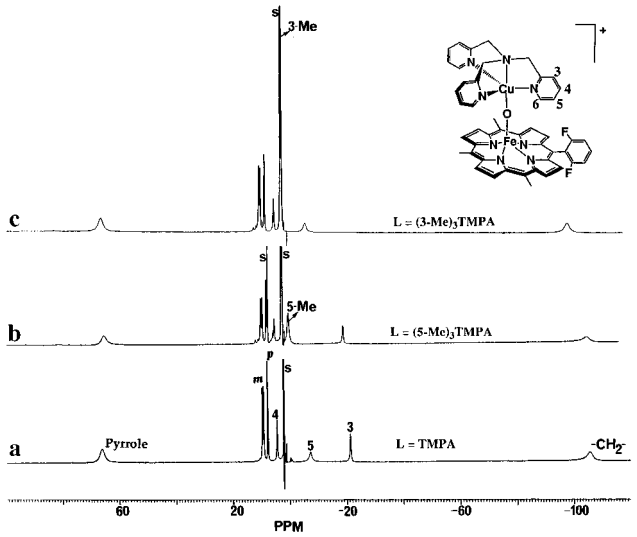

Figure 4. NMR spectrum of (a) [(F$_8$-TPP)Fe−O−Cu(TMPA)](ClO$_4$), (b) [(F$_8$-TPP)Fe−O−Cu((5-Me)$_3$-TMPA)](ClO$_4$), and (c) [(F$_8$-TPP)Fe−O−Cu((3-Me)$_3$-TMPA)](ClO$_4$) (CD_3CN, 295 K).

for the ^{1}H-NMR spectrum of [(F$_8$-TPP)Fe−O−Cu(TMPA)]$^+$ (**1**), discussed below, are summarized in Figure 3 and Table 1. The downfield-shifted signals are due to the Fe(III)−porphyrinate protons (Figure 4a).[8,10] The split-*meta* pair of the *meso*-phenyl substituents appears at δ 9.6 and 9.2 ppm, and the *p*-phenyl proton at $\delta \approx 7.8$ ppm, as is typical for tetraaryl porphyrinates. The broad pyrrole proton resonance is observed at $\delta \approx 65$ ppm (confirmed by deuteriation);[10] the downfield shift occurs through a σ contact mechanism which delocalizes unpaired spin in the $d_{x^2-y^2}$ orbital on to the pyrroles, via the Fe−N bonds.[2] This pyrrole peak, however, occurs in an upfield position (65 ppm) relative to other axially symmetric high-spin $S = 5/2$ (TPP)Fe(III)X (X = axial ligand) complexes, which typically appear at ca. 80 ppm.[2] Since the magnitude of the contact shift generally attenuates with lower net susceptibility, a pyrrole resonance at $\delta \approx 65$ ppm is consistent with a reduced total spin value of $S = 2$. This observation is in line with our earlier Mössbauer (solid state) and magnetic (solution and solid state) studies.[8]

In the downfield region, the ^{1}H-NMR spectra of the μ-oxo complexes [(F$_8$-TPP)Fe−O−Cu((*n*-Me)$_3$-TMPA)]$^+$ ($n = 3$, 4, and 5), as well as [(F$_8$-TPP)Fe−O−Cu(TMPA)]$^+$ (**1**), are essentially invariant with respect to the pyrrole ($\delta \approx 65$ ppm), and the *m*- and *p*-phenyl protons (Figure 4, Table 1). Methylation of TMPA, therefore, does not significantly affect the "electronics" of the [(F$_8$-TPP)Fe−O−Cu(L)]$^+$ system; comparison of the upfield regions (Figure 4) of [(F$_8$-TPP)Fe−O−Cu((*n*-Me)$_3$-TMPA)]$^+$ with **1**, therefore, convincingly reveals how a particular methyl substituent in [(F$_8$-TPP)Fe−O−Cu((*n*-Me)$_3$-TMPA)]$^+$ correlates with a peak due to a particular TMPA hydrogen in **1**, while unsubstituted pyridyl positions remain

(20) Kluiber, R. W.; Horrocks, W. D. *Inorg, Chem.* **1967**, *6*, 1427−1429.

unaffected, and appear in the same place. The spectrum of **1** displays four peaks accountable to the TMPA ligand; the three assigned by methylation appear at 4.5 (4-H), −7 (5-H), and −21 (3-H) (Table 1). New peaks expected for the methylated complex derivatives do appear (Figure 4, Table 1), and they correlate by integration to the anticipated "3-H" of a methyl substituent versus the "1-H" of the analogous position in TMPA.

For the (n-Me)$_3$-TMPA (n = 3, 4, and 5) free ligands, the Me protons appear at ∼2.5 ppm in each case. Since the methyl peaks in [(F$_8$-TPP)Fe−O−Cu((n-Me)$_3$-TMPA)]$^+$ (n = 3, 5) are upfield shifted (Table 1), this implies that any contribution from π contact shift sources is minimal, because a reversal in the sign and magnitude of the chemical shift of the methyl protons is expected for a predominantly π contact shift mechanism.[20] Furthermore, sign reversal of chemical shifts for the alternate pyridyl proton resonances would be expected for π contact spin delocalization.

Attenuation of the chemical shift with distance (through bonds) from the paramagnetic metal center is generally observed for a σ contact shift mechanism.[5] It is notable that the 4-Me protons are actually downfield shifted (to 7 ppm) for [(F$_8$-TPP)-Fe−O−Cu((4-Me)$_3$-TMPA)]$^+$; here, as in the case of [Cu((4-Me)$_3$-TMPA)]$^{2+}$ mentioned earlier, we invoke a π effect that has become significant only because of diminution of the σ contact effect so far from the Cu(II) center. The pyridyl 4-H signal, however, is upfield shifted, although much less so than the 3-H and 5-H (Table 1), which are one bond closer to Cu-(II). Thus, we conclude that σ contact shift dominates the spin delocalization mechanism in the TMPA moiety of [(F$_8$-TPP)-Fe−O−Cu(TMPA)]$^+$.

The slight upfield shift of the pyridyl 3-H relative to the pyridyl 5-H resonance may be due to some spin delocalization through the methylene bridge on to the pyridyl 3-H position in addition to spin density transmission via the Cu−N (pyridyl) bond. The observed line widths and T_1 (spin−lattice or longitudinal relaxation time) values for the 5-pyridyl (FWHM ≈ 500 Hz, T_1 = 1 ms) and 3-pyridyl (FWHM ≈ 150 Hz, T_1 = 5 ms) (FWHM = full width at half-maximum) protons suggest that the 5-pyridyl proton (also the 6-H(D), vide infra), due to its closer proximity, is experiencing an enhanced effect of the dipolar interaction (from the half-filled $d_{xz,yz}$ orbitals of the Fe-(III)−porphyrinate moiety) as well as ring current effects from the porphyrin moiety. The contribution from ring current effects to the observed chemical shifts is generally small, however, especially when compared with the magnitude of contact chemical shifts.[21]

Utilizing ^{2}H-NMR spectroscopy, the unambiguous assignment of the $-CD_2-$ protons of the tripod "arms", and the pyridyl 6-D, was achieved (Figures 5 and 6, Table 1). By comparison of [(F$_8$-TPP)Fe−O−Cu(TMPA)]$^+$ (Figure 5a) and [(F$_8$-TPP-d_8)Fe−O−Cu(($-CD_2-$)$_3$-TMPA)]$^+$ (Figure 5b), we deduce that it is the peak at −104 ppm which originates from the $-CD_2-$; the close proximity of the Cu(II) metal center accounts for its relative broadness.[4c] The chemical shift of the methylene proton resonance is also sensitive to solvent (−100 ppm in dichloromethane, −104 ppm in CD_3CN, −95 ppm in $(CD_3)_2CO$), perhaps because unpaired spin can be delocalized through hydrogen bonding interactions with solvent.

The μ-oxo complex [(F$_8$-TPP-d_8)Fe−O−Cu((6-D)$_2$-TMPA)]$^+$ was synthesized, this possessing two of three pyridyl 6-positions of TMPA and all of the pyrrole β-positions deuteriated. The ^{1}H- and ^{2}H-NMR spectra of this compound are shown (Figure 6) at two different temperatures (295 and 310 K); it is apparent

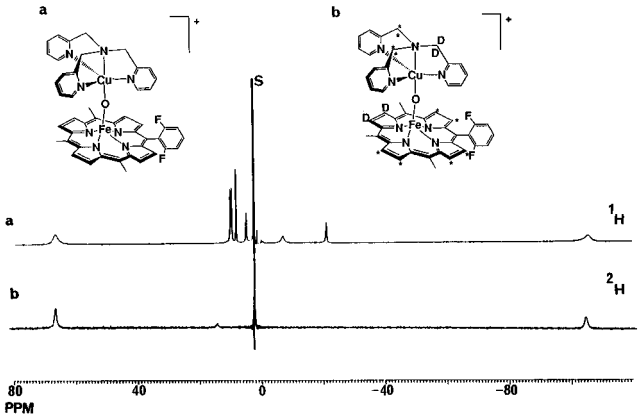

Figure 5. (a) ^{1}H-NMR spectrum of [(F$_8$-TPP)Fe−O−Cu(TMPA)]-(ClO$_4$), CD_3CN. (b) ^{2}H-NMR spectrum of [(pyrr-d_8)(F$_8$-TPP)Fe−O−Cu((-CD$_2$)$_3$-TMPA)](ClO)$_4$, CH_3CN, 295 K.

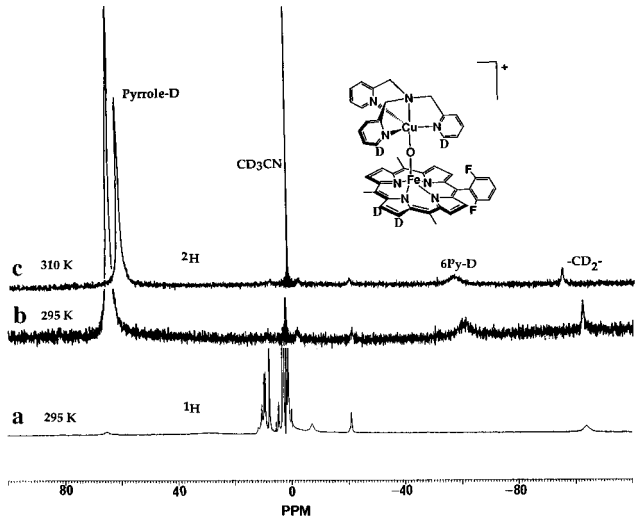

Figure 6. NMR spectra of [(pyrr-d_8)(F$_8$-TPP)Fe−O−Cu((6-D)$_2$-TMPA)](ClO)$_4$: (a) ^{1}H-NMR spectrum at 295 K, CD_3CN, (b) ^{2}H-NMR spectrum at 295 K, CH_3CN, (c) ^{2}H-NMR spectrum at 310 K, CH_3CN.

that a small, but detectable, amount of deuterium is also incorporated at the methylene (104 ppm) and 3-pyridyl (−21 ppm) positions of the TMPA moiety during the synthetic procedure. The single pyrrole D resonance at 65 ppm (295 K) and the hitherto unseen broad signal at −61 ppm, originating from the pyridyl 6-D, constitute the only appreciable signals for [(F$_8$-TPP-d_8)-Fe−O−Cu((6-D)$_2$-TMPA)]$^+$ (Figure 6b). This latter signal is quite broad (∼1000 Hz), and moves to −57 ppm upon warming to 310 K (Figure 6c), thus confirming that it is part of the paramagnetic complex, and not there as an instrumental artifact. The close proximity to the Cu(II) metal center, as well as to the quadrupolar pyridyl ^{14}N atom, probably accounts for the considerable broadening of the pyridyl 6-D, and explains why the corresponding peak is not seen in the ^{1}H-NMR spectrum.

Dynamic Behavior. The solution ^{1}H-NMR spectra of **1** ($CDCl_2/CD_3CN$) display dynamic behavior. From the crystal structure,[8] the mirror plane containing the Fe−O−Cu bond and one of the pyridyl groups of TMPA generates four unique pyrrole hydrogens, and renders the other two pyridyls equivalent. If this structure were retained in solution, we would expect four pyrrole signals of equal intensity, and two signals for each hydrogen of TMPA, in the ratio of 2:1. We see no such differentiation for any TMPA or porphryin pyrrole resonance, however, and attribute the loss of mirror symmetry to rapid rotation of the Cu(TMPA) moiety around the Cu−O bond, in addition to fluxionality of the Cu(II) center rapidly intercon-

(21) Scheer, H.; Katz, J. J. In *Porphyrins and Metalloporphyrins*; Smith, K. M., Ed.; Elsevier: New York, 1975; Chapter 10, pp 399−524.

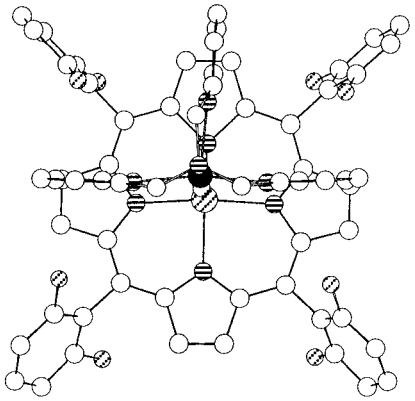

verting the Cu−N bonds, which forces all three pyridyls to become equivalent on the NMR time scale.

Effects of Antiferromagnetic Coupling in $S = 5/2$, $S = 1/2$ Fe−O(H)−Cu. In principle, the $S = 5/2$ and $S = 1/2$ spins couple to yield $S = 3$ (ferromagnetic) and $S = 2$ (antiferromagnetic) electronic states; the energy separation of these states ($2J$) is a measure of the coupling strength. As we describe below, it is the presence of strong antiferromagnetic coupling between high-spin Fe(III) and Cu(II) in **1** and **2** which is responsible for their very unusual ^{1}H-NMR spectroscopic behavior.

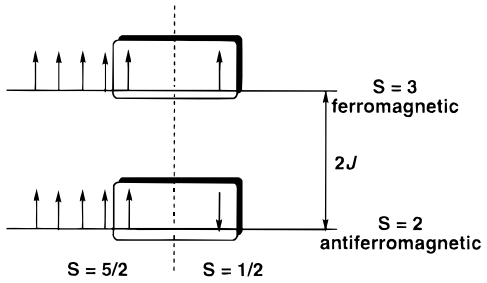

The hyperfine shift experienced by a nucleus in an exchange coupled system of the type M1···X···M2 (e.g., M1 = Cu, M2 = Fe, X is the bridging oxo ligand), such as those studied by Bertini, Luchinat, and co-workers, is given by the following general relationship:[5,12,15]

$$\Delta\nu/\nu_o = -(g_e\mu_B/3h\gamma_N\kappa T)\sum A_i\langle S_{iZ}\rangle \qquad (1)$$

where S_{iZ} is the expectation value evaluated over all the S_i states ($S = 2$ and $S = 3$) and averaged according to multiplicity ($2S_i + 1$) and Boltzmann population; the other symbols have their usual meaning.[12] A_i is the isotropic hyperfine coupling constant between a ligand hydrogen nucleus and spin state S_i ($S = 2$ or $S = 3$) for both metals. If we assume the hydrogen nucleus to interact with only one metal (e.g., Cu), the hyperfine coupling constant A_{Cu} can be related to A_i as follows:

$$A_i = A_{Cu}C_{iCu} \qquad (2)$$

where C is a coefficient which factors the coupling constant in the absence of coupling (A_{Cu}) to each S_i state. For an $S = 5/2$ (Fe) and $S = 1/2$ (Cu) antiferromagnetically coupled system the coefficients associated with the $S = 2$ (ground state) and $S = 3$ (excited state) have been determined to be $-1/6$ and $1/6$, respectively, for interaction of a ligand hydrogen nucleus with the Cu ion.[12] The corresponding values for interaction of the porphyrin hydrogen nucleus with Fe are $7/6$ and $5/6$, respectively. Hence, the only negative coefficient C is that for protons sensing Cu(II) and the $S = 2$ ground state. If the antiferromagnetic coupling is strong (i.e., separation between the $S = 2$ and $S = 3$ states is large), the contribution from the higher excited state ($S = 3$) would be minimal and a reversal in the sign of A_i (isotropic shift) for protons sensing Cu(II) is expected. This will be manifested as upfield-shifted peaks, as observed for **1**.

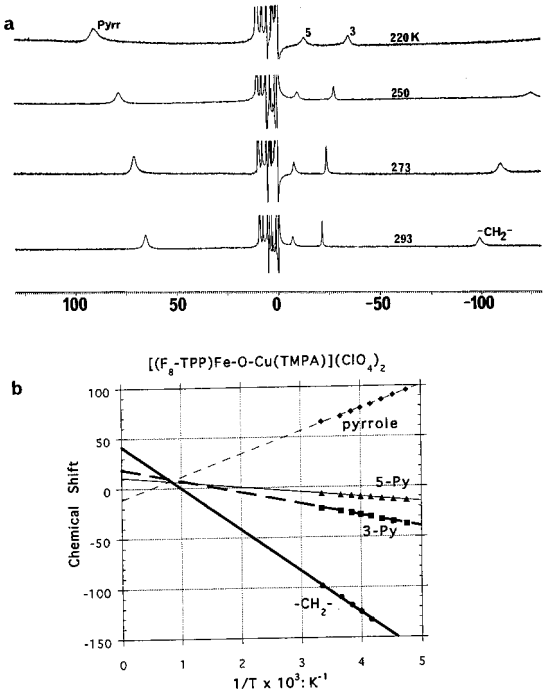

Figure 7. (a) Variable temperature ^{1}H-NMR spectra and (b) Curie plot (chemical shifts vs $1/T$) for [(F_8-TPP)Fe−O−Cu(TMPA)](ClO_4) in CD_2Cl_2.

Accordingly, for the antiferromagnetically coupled heterodinuclear Fe(III)−O−Cu(II) unit of **1**, the dramatically upfield-shifted profile of the TMPA protons indicates strong coupling.[12] For less strongly coupled systems, where mixing of the $S = 3$ state would be significant at room temperature, lowering of the temperature would be required to observe the reversal in chemical shifts.

For scalar coupling (through bonds), the gain or enhancement of the rate of electronic relaxation (τ_s) for Cu due to an antiferromagnetic coupling interaction with Fe is related to the square of the coupling constant, J.[12] A limit will be reached when the τ_s values for both metals become equal. In general, a small coupling ($J \approx -10$ cm^{-1}) is sufficient to reach this limit in the electronic relaxation rate for the slower relaxing metal ($\tau_s \approx 10^{-9}$ s).[12] Through scalar coupling ($J = -87$ cm^{-1} from solid state measurements[8]) with the faster relaxing metal (high-spin Fe(III) ($\tau_s \approx 10^{-11}$ s)), the enhanced electronic relaxation of Cu^{2+} results in much sharper proton NMR signals for the TMPA moiety of complex **1**, relative to the mononuclear Cu(II)TMPA species, and allows the observation of all signals except the pyridyl 6-H protons. As mentioned in the Introduction, there are examples of paramagnetic metal complexes having other than $S = 2$ ground states (homo- or heterobinuclear, and polynuclear species originating from nature or chemical synthesis), which also exhibit enhanced ligand peaks in their ^{1}H-NMR spectra due to magnetic coupling.

Variable Temperature (VT) NMR Studies. Figure 7b shows the effect of lowering the temperature on the NMR spectra of μ-oxo-bridged complex [(F_8-TPP)Fe−O−Cu(TMPA)]$^+$ (**1**). As shown, the upfield-shifted signals move further upfield while the downfield-shifted signals move further downfield, with broadening. The plots of chemical shift vs $1/T$

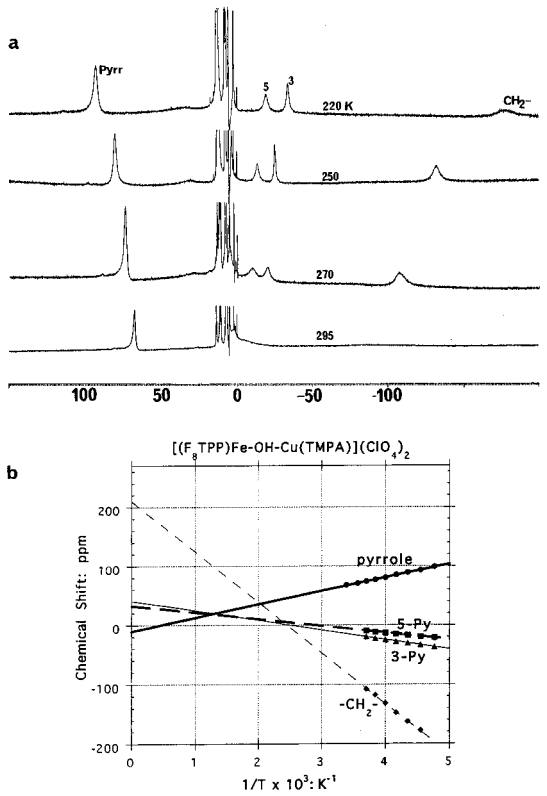

Figure 8. (a) Variable temperature ^{1}H-NMR spectra and (b) Curie plot (chemical shifts vs $1/T$) for [(F_8-TPP)Fe−OH−Cu(TMPA)](ClO_4)$_2$ in CD_2Cl_2.

(Figure 7a) show linear Curie and anti-Curie (or pseudo-Curie) behavior (in the temperature range 210−310 K) for the iron−porphyrinate and Cu(TMPA) protons, respectively, of **1**, consistent with strong antiferromagnetic coupling.[12] Note that the TMPA proton upfield-shifted signals all have associated positive (i.e., downfield) extrapolated intercepts, consistent with the breaking of the strong antiferromagnetic coupling as T approaches infinity: theoretically, the system uncouples[12] to behave as a Cu(II) mononuclear complex, such as [Cu(TMPA)(CH_3CN)]$^{2+}$ or here formally [Cu(TMPA)(O^{2-})]. Large extrapolated intercepts for Curie plots of pyrroline protons in iron(III) chlorin π-cation radical complexes have been reported where high-spin iron(III) ($S = 5/2$) is antiferromagnetically coupled with the $S = 1/2$ radical spin.[22]

As mentioned previously, the μ-oxo complex [(F_8-TPP)Fe−O−Cu(TMPA)]$^+$ (**1**) is quite basic and is readily protonated to yield μ-hydroxo complex [(F_8-TPP)Fe−OH−Cu(TMPA)]$^{2+}$ (**2**).[9,10] In its own right, **2** displays unusual ^{1}H-NMR spectra; for example, the position of the pyrrole peak is quite sensitive to solvent and counterion,[10] suggesting that potential hydrogen bonding interactions with the μ−OH species influence the extent of antiferromagnetic coupling, and hence the pyrrole peak position.

Figure 8a,b shows the effect of changing the temperature on the NMR spectra of the μ-hydroxo-bridged complex [(F_8-TPP)Fe−OH−Cu(TMPA)]$^{2+}$ (**2**). At lower temperatures (below 270 K) the NMR spectra of the μ-oxo- and μ-hydroxo-bridged complexes **1** and **2** exhibit similar chemical shift profiles (i.e., peak positions and line widths). We can therefore assign resonances in **2** to the same as those assigned for **1** (Table 1). The pyrrole assignment was confirmed by ^{2}H-NMR spectroscopy, and the position of this peak and magnetic properties of **2**[10] also argue for a $S = 2$ electronic ground state.[23] Figure 8a provides plots of chemical shift vs $1/T$ for the temperature range 295−210 K for the proton NMR resonances associated with **2**. The upfield-shifted signals all have positive extrapolated intercepts, in fact greater than those seen in [(F_8-TPP)Fe−O−Cu(TMPA)]$^+$ (**1**). The methylene proton resonance shows the largest variation with temperature for **2**, with a greater slope and intercept (220 ppm for **2** vs 40 ppm for **1**). The latter may be attributed to the different electronic environments around the Cu(II) center (i.e., in the hypothetically uncoupled mononuclear [Cu(TMPA)(X)]$^{n+}$), due to coordination of the monoanionic hydroxo versus dinegative oxo fifth ligand. For both complexes, the large chemical shift changes upon variation of temperature are consistent with a σ contact shift mechanism.[4c]

The difference in the chemical shift between the 3- and 5-pyridyl proton NMR resonances is less for [(F_8-TPP)Fe−OH−Cu(TMPA)]$^{2+}$ (**2**) relative to [(F_8-TPP)Fe−O−Cu(TMPA)]$^+$ (**1**) throughout the temperature range studied (Figures 7b and 8b and Table 1). In **1**, the relative downfield shift of the 5-pyridyl proton resonance vs the 3-pyridyl proton resonance was at least partially attributed to dipolar interaction with the iron porphyrin center (see earlier discussion). For the μ-hydroxo complex **2** with elongated Fe−(OH)− bond, the 5-pyridyl proton is expected to be further from the porphyrin plane, thus rendering it less susceptible to ring current effects and iron-centered dipolar interactions.

At 298 K, the pyrrole signal for [(F_8-TPP)Fe−OH−Cu(TMPA)][ClO_4]$_2$ (**2**−(ClO_4)$_2$) appears at 68.5 ppm, but the upfield signals associated with TMPA disappear. We propose that the relatively weak M−(OH) bonds result in partial dissociation of [(F_8-TPP)Fe−OH−Cu(TMPA)]$^{2+}$, in equilibrium with [(F_8-TPP)]Fe(III)OH and [Cu(TMPA)(ClO_4)$_2$]. It is plausible, however, that some [(F_8-TPP)Fe(III)ClO_4] is formed since, in a separate experiment, the addition of [(F_8-TPP)]Fe(III)OH to **2** results in the immediate appearance of some [(F_8-TPP)Fe−O−Fe(F_8-TPP)].[25] The rate of formation of [(F_8-TPP)Fe−O−Fe(F_8-TPP)] is very slow in the absence of added [F_8-TPP)Fe(III)OH], or moisture. There is precedent for NMR line widths being influenced by exchange with Cu(II)-ligand sites.[26,27] The lability of **2** undoubtedly diminishes considerably at lower temperatures, stabilizing the OH^- bridge, and allowing the electronic relaxation enhancement rate term to dominate the correlation time, and determine the nuclear relaxation rate and line widths.[5,12,15] Thus, as explained for complex **1**, the upfield-shifted peaks become detectable.

Conclusion

Proton NMR spectra of mononuclear [Cu(TMPA)(CH_3CN)]$^{2+}$ complexes showed the presence of a broad unresolved signal due to the 3- and 5-pyridyl resonances at ∼30 ppm and a

(22) Ozowa, S.; Watanabe, Y.; Morishima, I. *J. Am. Chem. Soc.* **1994**, *116*, 5832−5838.

(23) Direct comparisons of the room temperature magnetic moments of **1** and **2** provide $\mu_B = 5.1 \pm 0.1$ and $\mu_B = 5.5 \pm 0.1$, respectively, indicating a weaker magnetic interaction between bent Fe^{III}−OH−Cu^{II} (**2**, with longer M−O(H) bonds) compared to linear Fe^{III}−O−Cu^{II} in **1**.[10] A value of 6.2 μ_B is expected for an uncoupled Fe^{III}−Cu^{II} system. The observation of greater chemical shifts for comparable porphyrinate resonances in **2** vs **1** (Table 1) is also consistent with greater paramagnetism and weaker coupling in **2**. Weaker coupling compared to a related μ-oxo complex has been established by Holm and co-workers for μ−OH^- $S = 2$ complex [(OEP)Fe−OH−Cu(Me_5dien)($OClO_3$)]$^+$ ($J = -80$ cm^{-1}) (OEP = octaethylporphyrinate(2−); Me_5dien = 1,1,4,5,5-pentamethyldiethylenetriamine).[24]

(24) Scott, M. J.; Zhang, H. H.; Lee, S. C.; Hedman, B.; Hodgson, K. O.; Holm, R. H. *J. Am. Chem. Soc.* **1995**, *117*, 568−569.

(25) Nanthakumar, A. Ph.D. Dissertation, University of Iowa, Iowa City, IA, 1990.

(26) Espersen, W. G.; Hutton, W. C.; Chow, S. T.; Martin, R. B. *J. Am. Chem. Soc.* **1974**, *96*, 8111−8112.

(27) Esperson, W. G.; Martin, R. B. *J. Am. Chem. Soc.* **1976**, *98*, 40−44.

relatively sharp signal at 10.5 ppm due to the 4-pyridyl proton. In contrast, the structurally similar mononuclear $[Co(TMPA)(CH_3CN)]^{2+}$ complex exhibits well-separated and sharp NMR signals, in accord with known electronic relaxation properties of high-spin cobalt(II) complexes, compared to copper(II). The chemical shift profiles of mononuclear Co and Cu−TMPA complexes are each in agreement with a predominant σ contact shift mechanism.

The observed room temperature and variable temperature chemical shifts of $[(F_8\text{-TPP})Fe-O-Cu(TMPA)]^+$ (**1**) and $[(F_8\text{-TPP})Fe-OH-Cu(TMPA)]^{2+}$ (**2**) are also consistent with a predominant σ contact shift mechanism. Linear Curie plots of the respective pyrrole and TMPA chemical shifts (from 220 to 300 K for **1** and from 220 to 270 K for **2**) are consistent with a pure spin state, in each case $S = 2$, which derives from antiferromagnetic coupling of Cu(II) to high-spin Fe(III). The observance of this single spin state at room temperature for **1** indicates that the coupling is strong. In both **1** and **2**, this coupling is responsible for (a) enhancement of the electronic relaxation rate for Cu(II) and the consequent sharp proton NMR signals of the Cu(TMPA) moiety and (b) the upfield shift of the TMPA protons. The strikingly large magnitude of these upfield shifts further illustrates the strength of the coupling interaction in the heterobinuclear complex, and serves to define the prototypical ^{1}H-NMR spectroscopic signature of heme−copper complexes with an $S = 2$ ground state. The TMPA protons of **1** were assigned by specific methylation/deuteriation.

A logical development of this work is to probe further the relationship among magnetic coupling, NMR spectroscopic signatures, and the structural and other spectroscopic properties of the heterobinuclear moiety, $Fe^{III}-X-Cu^{II}$, through the synthesis and study of analogous complexes where X includes other ligands of possible biological relevance.

Acknowledgment. We thank the National Institutes of Health for support of this research and Professors Ivano Bertini and Claudio Luchinat (University of Florence) for encouragement and helpful discussions.

Supporting Information Available: Preparative details for the ligands and complexes, Figure S-1 with comparison of ^{1}H-NMR spectra of the $[Cu(TMPA)(CH_3CN)](ClO_4)_2$ complex with $[Cu((4\text{-}Me)_3TMPA)(CH_3CN)](ClO_4)_2$, and X-ray structure report for $[(TMPA)Co(II)(CH_3CN)](ClO_4)_2$, including experimental details, listing of atomic coordinates, temperature factors, and anisotropic temperature factors, and tables of bond lengths and bond angles (29 pages). See any current masthead page for ordering and Internet access instructions.

JA962404Q